

121.06, 29.51*, 31.14*, 26.11**, 26.55**, 27.08**, 26.55**, 36.58 (*t*-Bu), 29.81 ppm (*t*-Bu) (no other isomer detectable).

Compound **5** was obtained by reaction of 10 mL of 1 M (10 mmol) B_2H_6 solution in THF with 0.63 g (3.8 mmol) of olefin at 0 °C for 3 h, addition of 20 mL of H_2O , 20 mL of 3 N NaOH, and 20 mL of H_2O_2 (30%), extraction with pentane (2×50 mL), and distillation (57% yield). GLC showed the presence of two epimers (I and II) in $27 \pm 4\%$ and $73 \pm 4\%$ yields which were separated on a silica gel column (180×2.5 cm) with chloroform. Anal. ($C_{12}H_{24}O$, I and II) C, H.

1H NMR ($CDCl_3$) for I δ 0.94 (*t*-Bu); 3.83 ppm, $b_{1/2} = 14$ Hz (H_x); for II δ 0.85 (*t*-Bu); 3.98 ppm, $b_{1/2} = 10$ Hz (H_x).

^{13}C NMR (5–10% in $CDCl_3$ with 10% C_6F_6) C1–C10 for I 71.82, 54.01, 31.33*, 26.84**, 23.07**, 26.19**, 26.71**, 33.02*, 36.86 (*t*-Bu), 28.27 ppm (*t*-Bu); for II 70.39, 41.86, 34.06*, 29.18**, 23.33**, 26.52**, 27.36**, 37.31*, 35.16 (*t*-Bu), 26.91 ppm (*t*-Bu).

Solvolysis rates were determined automatically²⁴ by continuous titra-

tion with 0.015 N NaOH in 80% ethanol to pH 7.

Acknowledgment. We thank the Deutsche Forschungsgemeinschaft and the Fonds der Chemischen Industrie, Frankfurt, for financial support and Mrs. R. Links for skilful performance of many experiments. Linguistic help by Professor M. R. F. Ashworth is gratefully acknowledged.

Supplementary Material Available: IR and 1H NMR spectra of the separated epimers **2** and **3** ($X = OH$), ^{13}C spectrum of a mixture of **2** and **3** ($X = OH$), and 2H NMR spectrum of a solvolysis mixture (4 pages). Ordering information is given on any current masthead page.

(25) Note Added in Proof: J. E. Nordlander et al. have observed similar stereoselective reactions by using deuterated cyclooctyl sulfonates. We thank Professor Nordlander for communicating the results prior to publication and discussions.

(24) Schneider, H.-J.; Schneider-Bernlöhner, H.; Hanack, M. *Justus Liebig's Ann. Chem.* 1969, 722, 234.

Kinetic Isotope Effect Study of the Solvolysis of Neophyl Arenesulfonates¹

Takashi Ando,*† Seung-Geon Kim,^{2a†} Kenichi Matsuda,† Hiroshi Yamataka,† Yasuhide Yukawa,† Arthur Fry,† David E. Lewis,^{2b†} Leslie B. Sims,*† and Joe C. Wilson^{2c†}

Contribution from the Institute of Scientific and Industrial Research, Osaka University, Suita, Osaka 565, Japan, and the Department of Chemistry, University of Arkansas, Fayetteville, Arkansas 72701. Received March 10, 1980

Abstract: Carbon-14 and deuterium kinetic isotope effects (KIE) have been determined in the solvolysis reactions of para-substituted neophyl arenesulfonates. Large α -carbon KIE [1.094 in acetic acid (AcOH), 75 °C; 1.141 in trifluoroacetic acid (F_3AcOH), 0 °C] and medium Ph-1-carbon KIE (1.023 in AcOH; 1.035 in F_3AcOH) were observed for the unsubstituted neophyl brosylate; larger α -carbon and smaller Ph-1-carbon KIE were observed for a substrate with a more electron-donating substituent, and the reverse trend was found for electron-withdrawing substituents. These results, together with small β -carbon KIE (1.014 in AcOH and in F_3AcOH) and medium α -deuterium KIE (1.214 in AcOH; 1.247 in F_3AcOH , both per D_2), suggest that the reaction proceeds via a k_A mechanism in which the neighboring phenyl group participates in the rate-determining ionization step and that the transition state (TS) shifts to a more reactant-like structure as the electron-donating character of the substituent increases. The calculations of the KIE were carried out within the framework of transition state theory, in order to test these mechanistic conclusions, assuming a bridged TS structure with the neighboring phenyl group acting as an internal nucleophile displacing the leaving group. Cutoff models containing 10 atoms were used for both the reactant and TS, with structural parameters and force constants of the TS related to those of the reactant by empirical expressions relating geometry and force constants to bond orders. The bond orders of the five reacting bonds and a reaction coordinate consistent with S_N2 character at C_α constitute the independent parameters; consequently, families of solutions are found for which calculated KIE reproduce experimental values. The solutions are represented as regions on an O'Ferrall–Jencks reaction diagram; by requiring that the properties of the transition states vary smoothly with the Hammett σ parameter for substituents on the phenyl ring, a series of transition-state structures are found in which the C_α -leaving group bond is more than half-ruptured and the phenyl group is much less than half-transferred. The C_β -phenyl bond is largely intact and the C_α -phenyl bond develops at the expense of the π -electron density of the aromatic ring, similar to a bridged phenonium ion. The results are consistent with the qualitative nature of the transition state deduced from kinetic studies and provide strong support for the view that the neophyl arenesulfonates react via the k_A pathway.

Studies on neighboring-group participation in solvolysis reactions were initiated by Winstein^{3a} nearly four decades ago, and many studies have been carried out since then.^{3b,c} The 2-arylalkyl system, for which the term "anchimeric assistance" was first used,⁴ has been of special interest in this field. The question of whether the neighboring aryl group accelerates the solvolysis rate by anchimeric assistance in the 2-arylalkyl system has now been shown^{3b,c} to depend upon the structure, the substituents on the aromatic ring and at the β position, and the solvent. The 2-arylethyl sulfonates, the simplest of the 2-arylalkyl systems, have been shown to react either by an anchimerically assisted pathway (k_A) or by an

unassisted pathway (k_S) (Scheme I), depending upon the substituents R, the aromatic substituent, and the solvent. The first

(1) Part 11 of a series of neighboring group participation in solvolyses. For part 10, see Ando, T.; Yamawaki, J.; Saito, Y.; Yamataka, H. *Bull. Chem. Soc. Jpn.*, 1980, 53, 2348.

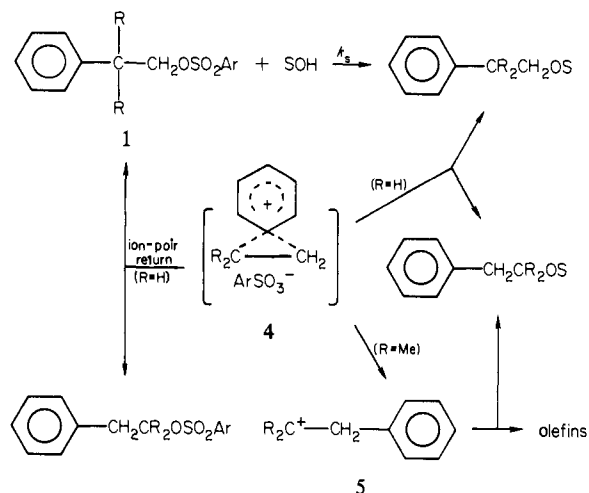
(2) (a) Department of Chemistry, Faculty of Science, Tokai University, Kitahana, Hirazuka 259-12, Japan; (b) Department of Chemistry, Baylor University, Waco, TX 76798. (c) BASF Wyandotte Corp., Wyandotte, MI 48192.

(3) (a) Winstein, S.; Lucas, H. J. *J. Am. Chem. Soc.* 1939, 61, 1576, 2845; (b) Capon, B. *Q. Rev. Chem. Soc. (London)* 1964, 45; (c) Lancelot, C. J.; Cram, D. J.; Schleyer, P. v. R. In "Carbonium Ions"; Olah, G. A., Schleyer, P. v. R., Eds.; Wiley: New York, 1972; Chapter 27.

(4) Winstein, S.; Lindgren, C. R.; Marshall, H.; Ingraham, L. L. *J. Am. Chem. Soc.* 1953, 75, 147.

† Osaka University.

† University of Arkansas.

Scheme I^a

^a R = H, 2-Phenylethyl; R = Me, neophyl.

definitive evidence of aryl group participation was the observation^{5,6} of normal carbon-14 kinetic isotope effects for labeling at phenyl-1 in the solvolysis of 2-arylethyl nosylates. Other kinetic evidence suggests that 2-(*p*-methoxyphenyl)ethyl tosylate in acetic acid and 2-phenylethyl tosylate in trifluoroacetic acid react predominantly via the k_A pathway, whereas 2-phenylethyl tosylate in acetic acid solvolyzes predominantly by the k_S pathway.^{3b,c}

There is considerable interest in investigating the structure of the transition state for the 2-arylethyl solvolysis in detail, since the transition state for the k_A process precedes the so-called phenonium ion intermediate whose structure has been a matter of long debate and also because the reaction itself is a unique rearrangement in which the neighboring aryl group plays the role of an intramolecular nucleophile displacing the leaving group. In order to obtain information concerning the structure of the transition state in this complex reaction, it is desirable to observe kinetic isotope effects for labeling at several different atoms in the reaction.⁷ However, these measurements are difficult in the 2-arylethyl solvolyses because of the presence of both aryl-assisted (k_A) and aryl-unassisted (k_S) pathways and because of the occurrence of ion-pair return resulting in scrambling of labels (Scheme I).

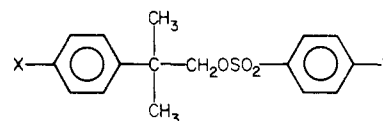
The neophyl (2-methyl-2-phenyl-1-propyl) esters (Scheme I, with R = Me) were chosen for this study. Introduction of two methyl groups on the β -carbon of the parent 2-phenylethyl esters enhances phenyl rearrangement and restricts direct attack of a solvent molecule at the α -carbon. Acetolysis of neophyl tosylate leads to completely rearranged products consisting largely of olefins and an ester arising from phenyl migration (>99%),^{8,9} introduction of a substituent on the phenyl ring in the neophyl system does not significantly affect the fraction of the aryl-assisted (k_A) pathway.^{10,11} Although the bridged phenonium ion (4) originally proposed by Winstein as an intermediate in the phenyl-assisted acetolysis of neophyl tosylate was questioned and the rearranged tertiary cation (5) was thought to be the first intermediate (Scheme I),^{12,13} kinetic behavior of the neophyl solvolysis ensures that the solvolysis can be regarded as a model of the k_A pathway as far

as the transition state is concerned.^{14,15} The major mechanistic difference in the k_A pathways for the neophyl and the 2-arylethyl systems is that for the neophyl system, the neighboring phenyl group migrates in a rate-determining step and ion-pair return from the carbocation is not kinetically important, whereas for the 2-arylethyl system, ion-pair return from the phenonium ion intermediate is important and therefore either formation or collapse of the intermediate could be rate determining. Despite these differences, however, other evidence suggests that the transition states for the two systems are essentially the same: (1) the values of ΔS^\ddagger are ~ 7.0 eu for both systems; values of ~ 15.0 eu are characteristic of k_S processes;¹⁶ (2) the response of rate to solvent ionizing power is the same for the two systems;¹⁴ (3) a plot of $\log k_A$ for the neophyl tosylate against $\log k_A$ for the corresponding para-substituted 2-phenylethyl tosylates is linear, with a slope of 0.98;¹³ (4) the observed kinetic isotope effects are similar in magnitude for the two systems at each of the positions C $_{\alpha}$, C $_{\beta}$, C $_{Ph-1}$, and D $_{\alpha}$ (vide infra). It thus appears that there is a transition state characteristic of k_A processes which differs from that for S $_N1$ and S $_N2$ processes. The neophyl esters thus provide good models for studying variations in transition-state structure for the k_A process.

In this paper, kinetic isotope effects in the acetolysis of substituted neophyl arenesulfonates are reported,^{11,18} and the experimental results are compared with those calculated for various transition-state models. The usefulness of this combined experimental-theoretical approach has been demonstrated for a few cases, including S $_N$ reactions^{19,20} and elimination reactions.^{21,22} In this paper, we extend this approach to rearrangement reactions.

Experimental Section

Materials. Neophyl alcohol was prepared by the Grignard oxidation²³ of neophyl chloride, which was obtained by the Friedel-Crafts reaction of benzene with 2-methylallyl chloride.²⁴ Esterification of the alcohol with *p*-bromobenzenesulfonyl chloride gave neophyl brosylate. The



- 1, X = H; Y = Br
- 2, X = Br; Y = Br
- 3, X = CH₃O; Y = CH₃

brosylate was also synthesized from benzoic acid in order to establish a synthetic route for the carbon-14-labeled compounds. Neophyl brosylates labeled with carbon-14 at the phenyl-1 (1-*Ph-1*-¹⁴C) and the β -carbon (1- β -¹⁴C) were prepared from benzoic-*1*-¹⁴C acid and benzoic-carbonyl-¹⁴C acid, respectively (obtained from the Radiochemical Centre). The benzoic acids were converted to dimethylphenylacetone nitriles via reduction, chlorination, cyanation, and dimethylation.²⁵ The nitriles were then hydrolyzed and reduced to give neophyl alcohol, which was finally converted to the desired esters by Tipson's method.²⁶ Neophyl- α -¹⁴C brosylate (1- α -¹⁴C) was synthesized with potassium cyanide-¹⁴C (obtained from New England Nuclear) as a carbon-14 source in the same series

(5) Yukawa, Y.; Ando, T.; Token, K.; Kawada, M.; Kim, S.-G. *Tetrahedron Lett.* **1969**, 2367.

(6) Yukawa, Y.; Ando, T.; Kawada, M.; Token, K.; Kim, S.-G. *Tetrahedron Lett.* **1971**, 847.

(7) Fry, A. *Pure Appl. Chem.* **1964**, 8, 409.

(8) Heck, R.; Winstein, S. *J. Am. Chem. Soc.* **1957**, 79, 3432.

(9) Saunders, W. H., Jr.; Paine, R. H. *J. Am. Chem. Soc.* **1961**, 83, 882.

(10) Tanida, H.; Tsuji, T.; Ishitobi, H.; Irie, T. *J. Org. Chem.* **1969**, 34, 1086.

(11) Wilson, J. C. Ph.D. Dissertation, University of Arkansas, Fayetteville, Arkansas, 1975.

(12) Brown, H. C.; Bernheimer, R.; Kim, C. J.; Scheppele, S. E. *J. Am. Chem. Soc.* **1967**, 89, 370.

(13) Fainberg, A. H.; Winstein, S. *J. Am. Chem. Soc.* **1956**, 78, 2763.

(14) Diaz, A.; Lazdins, I.; Winstein, S. *J. Am. Chem. Soc.* **1968**, 90, 6546.

(15) Schadt, F. L., III; Lancelot, C. J.; Schleyer, P. v. R. *J. Am. Chem. Soc.* **1978**, 100, 228.

(16) Winstein, S.; Heck, R. *J. Am. Chem. Soc.* **1966**, 78, 4801.

(17) Jones, M. G.; Coke, J. L. *J. Am. Chem. Soc.* **1969**, 91, 4284.

(18) Some of the results have appeared in communications form: (a) Yukawa, Y.; Kim, S.-G.; Yamataka, H. *Tetrahedron Lett.* **1973**, 373; (b) Yamataka, H.; Kim, S.-G.; Ando, T.; Yukawa, Y. *Ibid.*, 4767.

(19) Sims, L. B.; Fry, A.; Netherton, L. T.; Wilson, J. C.; Repoond, K. D.; Crook, S. W. *J. Am. Chem. Soc.* **1972**, 95, 1364.

(20) Burton, G. W.; Sims, L. B.; Wilson, J. C.; Fry, A. *J. Am. Chem. Soc.* **1977**, 99, 3371.

(21) Burton, G. W.; Sims, L. B.; McLennan, D. J. *J. Chem. Soc., Perkin Trans. 2* **1977**, 1763, 1847.

(22) Lewis, D. E.; Sims, L. B.; Yamataka, H.; McKenna, J. *J. Am. Chem. Soc.* **1980**, 102, 7411.

(23) Whitmore, F. C.; Weigerber, C. A.; Shabica, A. C., Jr. *J. Am. Chem. Soc.* **1943**, 65, 1469.

(24) "Organic Syntheses"; Wiley: New York, 1963; Collect. Vol. 4, p 702.

(25) Taranko, L. B.; Rerry, R. H., Jr. *J. Org. Chem.* **1969**, 34, 226.

(26) Tipson, R. S. *J. Org. Chem.* **1944**, 9, 235.

Table I. Experimental Kinetic Isotope Effects in the Solvolyses of Neophyl Esters

labeled position	substituent	leaving group ^a	temp, ^b °C	solvent ^c	10 ⁵ k, s ⁻¹	k/*k	ref
α- ¹⁴ C	<i>p</i> -CH ₃ O	OTs	50.00	AcOH	11.8 ± 0.1	1.117 ± 0.009	this work
			35.00	AcOH	2.10 ± 0.01	1.121 ± 0.003	this work
	<i>p</i> -H	OBs	75.00	AcOH		1.093 ± 0.003	18b
			0.02	F ₃ AcOH		1.141 ± 0.001	18b
	<i>p</i> -Br	OBs	100.00	AcOH		1.084 ± 0.001	this work
			85.00	AcOH		1.088 ± 0.001	this work
β- ¹⁴ C	<i>p</i> -H	OBs	75.00	AcOH		1.014 ± 0.001	18b
			0.02	F ₃ AcOH		1.014 ± 0.001	18b
Ph- <i>l</i> - ¹⁴ C	<i>p</i> -CH ₃ O	OBs	40.00	AcOH	13.2 ± 0.05	1.006 ± 0.001	10
			75.00	AcOH	6.99 ± 0.04	1.023 ± 0.001	18
	<i>p</i> -H	OBs	40.00	AcOH		1.031 ± 0.001	10
			0.02	F ₃ AcOH		1.035 ± 0.001	18
	<i>p</i> -Br	OBs	100.00	AcOH	15.9 ± 0.1	1.027 ± 0.001	this work
			85.00	AcOH	3.35 ± 0.01	1.030 ± 0.001	this work
α-D ₂	<i>p</i> -CH ₃ O	OMs	25.00	7OT		1.248	30
			25.00	7OT		1.254	30
	<i>p</i> -CH ₃	OMs	25.00	7OT		1.272	30
			75.00	AcOH		1.214 ± 0.002	18
	<i>p</i> -H	OBs	0.02	F ₃ AcOH		1.247 ± 0.008	18b
			25.00	7OT		1.286	30
	<i>m</i> -CF ₃	OTr	25.00	7OT		1.208	30
			25.00	7OT		1.208	30

^a OTs is *p*-toluenesulfonate; OBs is *p*-bromobenzenesulfonate; OMs is methanesulfonate; Tr is 2,2,2-trifluoroethanesulfonate. ^b ±0.01 °C. ^c AcOH is acetic acid; F₃AcOH is trifluoroacetic acid; 7OT is 70 wt % 2,2,2-trifluoroethanol-30% water.

of reactions. Introduction of deuterium at the α position of the neophyl ester (1-α-D₂) was achieved by use of lithium aluminum deuteride as the reducing agent. Preparation of the *p*-Br-substituted derivatives (2-*Ph-l*-¹⁴C and 2-α-¹⁴C) was achieved by bromination of labeled 2-phenyl-2-methylpropanoic acids, followed by a similar sequence of steps to those for the parent compound. The *p*-CH₃O ester labeled with carbon-14 at the α position (3-α-¹⁴C) was prepared by cyanation of *p*-methoxybenzyl chloride with potassium cyanide-¹⁴C, followed by the same route as described above. The chemical purity of the labeled compounds was verified by comparison of their physical constants and spectroscopic data with those for the unlabeled compounds. All ¹⁴C-labeled compounds had molar radioactivities of about 3–4 mCi/mol, and these were used without further dilution during the preparation procedures. The final neophyl esters were carefully purified by repeated recrystallization until the molar activities remained constant.

Kinetic Procedures. Acetic acid was refluxed over 2.0 wt % potassium permanganate for 8 h and fractionally distilled, and the middle cut was refluxed over triacetyl borate, followed by fractional distillation (bp 118.0–118.5 °C); the freezing point of 16.5 °C corresponds to 99.85% purity. Trifluoroacetic acid was purified by fractional distillation (bp 71.5–72.0 °C) from phosphorus pentoxide, followed by addition of 1.0 wt % freshly distilled trifluoroacetic anhydride. The solution was transferred into a screw-capped bottle and stored in a desiccator.

Acetolysis was followed by a method reported by Winstein.²⁷ The initial concentration of esters was 0.05 M. Titration was carried out by use of 0.051 M perchloric acid and 0.026 M sodium acetate in acetic acid as standard acid and base, respectively, and β-naphtholbenzein as an indicator. Rate constants in trifluoroacetic acid were determined by a UV method similar to that of Peterson²⁸ in which the absorbance of *p*-bromobenzenesulfonates at 249 nm was used to follow the reactions. The initial concentration of esters was 0.02 M. Data points measured were usually 12. Although the reaction solutions tended to have a slight color after 10 half-lives, the infinity absorbance was reasonably reproducible, and the first-order rate plots by use of the experimental infinity absorbance gave good straight lines with correlation coefficients better than 0.999 without any systematic drift.

Determination of Kinetic Isotope Effects. Reactions of carbon-14-labeled compounds were carried out in the same way as those of unlabeled compounds, except for the larger scale necessary to recover sufficient unreacted starting materials for the radioactivity determinations; the scale was shown to have no effect on the rate. To determine the kinetic isotope effects (KIE), we recovered the unreacted esters at several different fractions of reaction, ranging from 0 to 75% completion, purified them by recrystallization until constant activities were attained, and then assayed^{29a} them. For acetolysis, aliquots of the 0.05 M esters large enough

to yield sufficient unreacted starting material for assaying were delivered to individual ampules corresponding to preselected fractions of reaction, and the ampules containing the samples were sealed. For trifluoroacetolysis, the reaction sample was delivered to one-batch containers. The samples were then reacted by placing them in a constant temperature bath for a time sufficient to assure the desired fraction of reaction (determined from the kinetics of the unlabeled analogues) and quenched either by removing an ampule, breaking the seal, and pouring the contents into cold water (for acetolysis) or by withdrawing a sample from the batch reactor and delivering it into ice-water (for trifluoroacetolysis). The precipitates (unreacted esters) were filtered and purified by repeated recrystallization from ligroin (bp 100–120 °C).

The purified precipitates (5–10 mg) were oxidized in a modified Pregl micro combustion furnace, and the radioactive carbon dioxide gas generated was collected by passing dry air into an ionization chamber (250-mL capacity, Nuclear Chicago). The chamber was then set on a vibrating-reed electrometer (Takeda Riken TR-84M) which was connected to a digital voltmeter and a computer which averaged the ionization current measured at 10-s intervals for 40 min. The radioactivity of each sample was measured at least twice, resulting in a standard deviation usually less than 0.3%.

Kinetic isotope effects were then calculated by use of eq 1^{29b}

$$\log A_x = \log A_0 - [1 - (^{14}k/^{12}k)] \log(1 - x) \quad (1)$$

where *x* is the fraction of reaction, and *A*₀ and *A*_{*x*} are the molar activities of the initial and recovered ester, respectively. If eq 1 is written as *y* = *a* + *bx*, linear regression yields the slope *b* and the associated standard error Δ*b*. These are related to the isotope effect by

$$^{12}k/^{14}k = (1 + b)^{-1} \pm \Delta b / (1 + b)^2 \quad (2)$$

The data obtained for the acetolysis of 1-α-¹⁴C are plotted in Figure 1 as a typical example. The correlation coefficients for fit of the experimental activities to eq 1 were in the range 0.997–0.999. Deuterium isotope effects were determined by comparative experiments.

Results

The results for this reaction are summarized in Table I; activity data for the results obtained in this study are provided in the supplementary material. Values of the α-¹⁴C, β-¹⁴C, Ph-*l*-¹⁴C, and α-D₂ KIE for the parent compound (*p*-H substituent) were measured at 75 °C in AcOH. The α-¹⁴C KIE for other substituents were estimated from those in Table I by assuming a temperature dependence as in eq 3. For other cases, estimates

$$\log(k/*k) = A + B/T \quad (3)$$

(27) Winstein, S.; Hanson, C.; Grunwald, E. *J. Am. Chem. Soc.* **1948**, *70*, 812.

(28) Peterson, P. E.; Kelley, R. E., Jr.; Belloli, R.; Sipp, K. A. *J. Am. Chem. Soc.* **1965**, *87*, 5169.

(29) Raen, V. F.; Ropp, G. A.; Raen, H. P. "Carbon-14"; McGraw-Hill: New York, 1968; (a) Chapter 11; (b) Chapter 5.

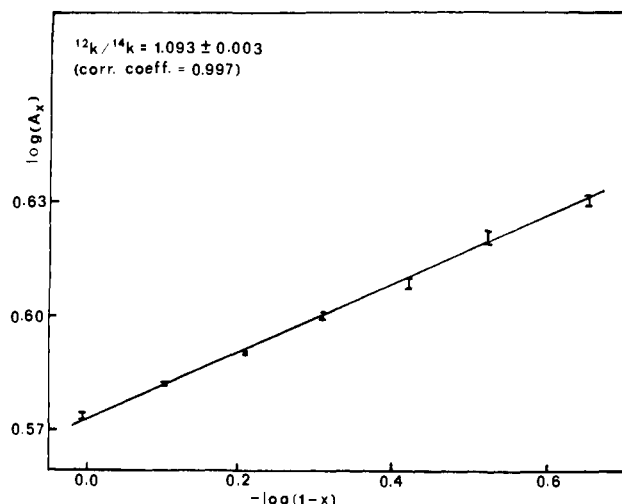


Figure 1. Plot of specific radioactivity of recovered ester vs. the fraction of reaction in acetolysis of neophyl- α - ^{14}C brosylate (**1**) at 75 °C.

of KIE at 75 °C were made as follows, using the phenyl- l - ^{14}C KIE as example: the KIE for substituents X at 40 °C are plotted against $\log(k_X/k_H)$ as the top line of Figure 2. A line through the experimental KIE for the parent compound at 75 °C and parallel to the 40 °C line provides a good estimate of the KIE at 75 °C for the other substituents. Similar estimates were made for the other measured KIE, providing the values of the KIE at 75 °C in acetic acid given in Table II. Although slight errors may be introduced into the KIE values by this method of estimation, we believe the trends in the KIE are real and that comparisons with KIE calculated for various transition-state models provide meaningful information on the nature of these processes.

The physically reasonable transition-state (TS) models to consider are suggested by a qualitative consideration of the magnitudes of the observed KIE. Normal kinetic isotope effects ($k/^*k > 1$) were observed for all positions, consistent with a k_A mechanism in which the phenyl group at the β position migrates in a rate-determining ionization step.^{3c} The phenyl- l - ^{14}C KIE has been measured for a number of rearrangements as shown in Table III. The present results (2.3% in AcOH at 75 °C and 3.5% in trifluoroacetic acid (F_3AcOH) at 0 °C for **1**) are within the range observed (2–5%) for reactions proved to proceed by a concerted mechanism; a null effect is observed for the nonconcerted Schmidt rearrangement. The results are also very similar in magnitude to those observed in solvolyses of 2-(2-methoxyphenyl)ethyl esters (2.8% in AcOH at 60 °C and 3.6% in F_3AcOH

Table II. Kinetic Isotope Effects in the Acetolysis of Para-Substituted Neophyl Esters at 75 °C

labeled position	substituent	leaving group	$k/^*k$
α - ^{14}C	<i>p</i> - CH_3O	OTs	1.111
	<i>p</i> -H	OBs	1.093
	<i>p</i> -Br	OBs	1.090
β - ^{14}C	<i>p</i> -H	OBs	1.014
	Ph- l - ^{14}C	<i>p</i> - CH_3O	1.006
	<i>p</i> -H	OBs	1.023
α - D_2	<i>p</i> -Br	OBs	1.032
	<i>p</i> -H	OBs	1.214

Table III. Phenyl- l - ^{14}C Kinetic Isotope Effects in Molecular Rearrangements

reaction	compounds	$^{12}\text{k}/^{14}\text{k}$	ref
Hofmann	<i>N</i> -chlorobenzamide	1.046	31
	<i>N</i> -bromobenzamide	1.044	32
Lossen	potassium benzoilbenzohydrozamate	1.032	32
Baeyer-Villiger	acetophenone	1.048	33
Wolff	1-(1-naphthyl)-3-diazo-2-propanone	1.015	32
	α -diazoacetophenone	1.00	34
Beckmann	acetophenone oxime	1.019–	35
		1.026	
Schmidt	acetophenone	1.00	36
Curtius	benzazide	1.042	32

at 0 °C),^{5,6} which supports the assumption that the neophyl solvolysis can be considered as a model of the k_A process for 2-phenylethyl ester solvolyses.

It is interesting that all of the phenyl- l - ^{14}C KIE are normal even though the trivalent sp^2 phenyl-1 position becomes a tetra-valent carbon in the transition state, so that formally the reaction corresponds to an addition at this position for which small normal, null, or even inverse ($k/^*k < 1$) KIE are expected (inverse isotope effects arise when the bonding at the labeled position increases during the reaction and would have abnormal temperature dependences). However, the observed KIE are normal and of medium magnitude and exhibit normal temperature dependences ($k/^*k$ decreases with increasing temperature) as can be seen in Table I. Therefore, the results suggest that the bonding at Ph-1 is actually decreasing during the reaction, consistent with partial C_β - C_{Ph} bond rupture and breakdown of aromaticity in the benzene ring in the bridged TS. Similar results have recently been reported for the Beckman rearrangement of acetophenone oxime.³⁵

The observed α -carbon-14 KIE, 1.09–1.14, are quite large and comparable to those reported for $\text{S}_{\text{N}}2$ reactions.^{37,38} However,

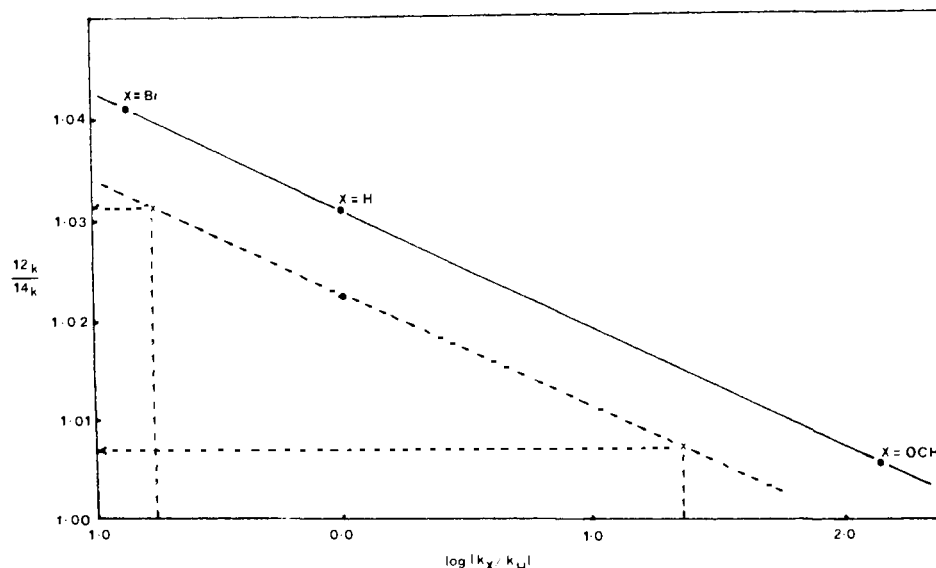


Figure 2. Estimation of Ph- l - ^{14}C kinetic isotope effect at 75 °C (---) from measured values at 40 °C (—).

the magnitudes of the α -deuterium KIE, 1.20–1.24 per D_2 , which are about the same as those reported for the related 2-phenylethyl system,^{30,39–41} are much larger than those for S_N2 and half the size of the limiting value observed for S_N1 reactions.^{42,43} The most plausible explanation of these results is that there is a unique transition state for k_A processes which is different from either an S_N1 transition state (which requires resonance and/or hyperconjugative stabilization by adjacent groups^{20,32,44}) or an S_N2 transition state (in which the nucleophile– C_α –leaving group forms a [probably] linear three-center moiety). Comparison of the magnitudes of the present observed α KIE and those for S_N1 and S_N2 processes leads to the likely assumption that the phenyl group acts as an internal nucleophile to displace the leaving group in an S_N2 -like displacement at C_α , but probably with much weaker nucleophile– C_α and C_α –leaving group bonding because of the high ionizing power of the solvent, high nucleofugacity of the sulfonate leaving group, and low nucleophilicity of the phenyl ring. It is also likely that the phenyl group is still significantly bonded to the β carbon, so that the $Ph-C_\alpha-H(D)$ angle must be larger than 90° in contrast to the usual S_N2 case, which would lead to smaller new bending force constants to the hydrogens²⁰ and, consequently, a larger deuterium KIE than normally observed for S_N2 reactions.

Little attention has been given to the bonding at the β carbon in the solvolysis of 2-arylalkyl esters, despite the possibility of a bridged, three-membered ring structure in the transition state. Saunders and co-workers measured the β -deuterium KIE in the solvolysis of 2-phenylethyl tosylate (**6**) and observed 1.00 for the k_A solvolysis in formic acid and 1.04 for the k_S solvolysis in acetic acid.^{40a} From these results, they concluded that there was no bonding change at the β carbon in the k_A transition state; however, such an interpretation is not required since a null KIE can also arise by a cancellation of factors favoring an inverse KIE (such as an inductive effect⁴⁵) and factors (such as bond breaking or hybridization changes) favoring normal KIE. The small but distinct β -carbon-14 KIE observed for the neophyl ester (1.014 in both AcOH and F_3AcOH) is conclusive evidence for a bonding change at the β carbon. The bonding change could be simply the transformation from an acyclic reactant to a cyclic TS without formal bond order changes, for example. Fractionation data calculated by Hartshorn and Shiner⁴⁶ yielded a carbon-13 isotope effect of 1.012 in the hypothetical equilibrium between propane-2- ^{13}C and cyclopropane- ^{13}C . Since carbon-14 isotope effects are about twice as large as carbon-13 effects, the observed β -carbon-14 isotope effect of 1.014 could result from a bridged TS structure approximately midway between the propane-cyclopropane transformation. However, Hartshorn and Shiner⁴⁶ also calculate a deuterium isotope effect of 1.074 per D_2 , a value too far removed from the value observed (1.00) for the 2-phenylethyl solvolysis^{40a} to be attributed to the difference between the neophyl and 2-phenylethyl systems, so that this explanation of the observed β -carbon KIE can be reasonably excluded. The most likely ex-

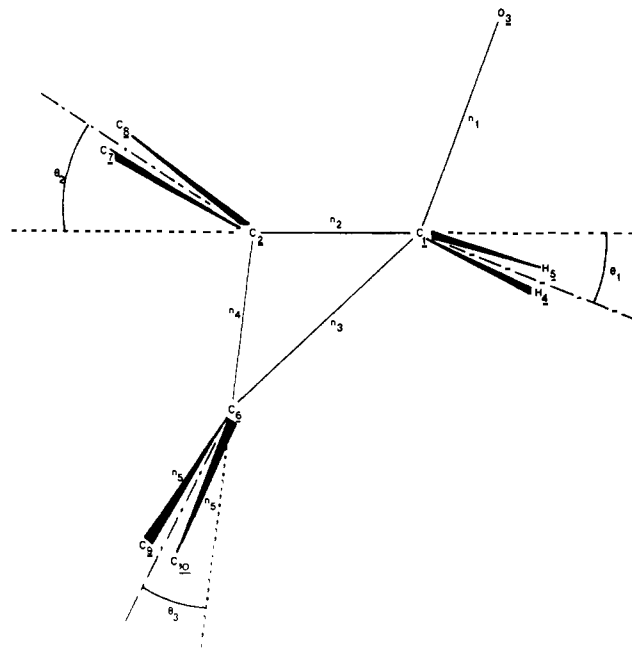
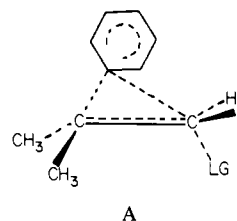


Figure 3. 10-Atom cutoff model for cyclic transition state.

planation of the observed β -carbon-14 KIE is thus a partial breaking of the $Ph-C_\beta$ bond, as the phenyl group begins to migrate to C_α in the k_A transition state.

Thus all of the results are consistent with a bridged transition state in which the phenyl group acts as an intramolecular nucleophile, with only slight $Ph-C_\beta$ bond rupture and slight geometry changes about C_β , weak $Ph-C_\alpha$ and C_α –leaving group bonds, and slight $C_\alpha-C_\beta$ double bond formation (structure A). Structure



A

A can be regarded as typical for the k_A solvolysis of 2-arylalkyl systems and was used as the transition-state model for the theoretical calculations described below. It is interesting to note here that the analogous transition-state structure in the solvolysis of 2-phenylethyl tosylate is reasonable as a precursor to the symmetrical phenonium ion intermediate, whose structure was estimated by molecular orbital calculations to have weak $C_{Ph}-C_{\alpha,\beta}$ bonds and a strong $C_\alpha-C_\beta$ bond.^{47,48}

Calculations

The initial model employed for both reactant and transition state was a 10-atom cutoff⁴⁹ model (Figure 3) in which only the carbons (C_7 and C_8) of the two β -methyl groups were retained; carbons C_6 , C_9 , and C_{10} represent the aromatic ring system; and the oxygen O_3 is retained as the cutoff for leaving sulfonate moiety. The conformation about the $C_\alpha-C_\beta$ bond is staggered, with the phenyl and leaving groups anti; the model, therefore, contains a plane of symmetry defined by atoms C_1 , C_2 , O_3 , and C_6 , which bisects the migrating phenyl group ($C_9C_6C_{10}$), two methyl groups (C_7 and C_8), and the two α -hydrogens (H_4 and H_5), in both the reactant and the transition state.

For the reactant, standard bond lengths,⁵⁰ r^0 , were employed for all bonds; tetrahedral geometry was assumed about the α and

- (30) Shiner, V. J., Jr.; Seib, R. C. *J. Am. Chem. Soc.* **1976**, *98*, 862.
 (31) Imamoto, T.; Kim, S.-G.; Tsuno, Y.; Yukawa, Y. *Bull. Chem. Soc. Jpn.* **1971**, *44*, 2276.
 (32) Fry, A. In "Isotope Effects in Chemical Reactions"; Collins, C. J.; Bowman, N. S., Eds.; Van Nostrand Reinhold: New York, 1970; Chapter 6.
 (33) Palmer, B. W.; Fry, A. *J. Am. Chem. Soc.* **1970**, *92*, 2580.
 (34) Yukawa, Y.; Ibata, T. *Bull. Chem. Soc. Jpn.* **1969**, *42*, 802.
 (35) Kim, S.-G.; Kawakami, T.; Ando, T.; Yukawa, Y. *Bull. Chem. Soc. Jpn.* **1979**, *52*, 1115.
 (36) Yukawa, Y.; Toriyama, T., unpublished results.
 (37) Bender, M. L.; Hoeg, D. F. *J. Am. Chem. Soc.* **1957**, *79*, 5649.
 (38) Buist, G. J.; Bender, M. L. *J. Am. Chem. Soc.* **1958**, *80*, 4308.
 (39) Saunders, W. H., Jr.; Asperger, S.; Edison, D. H. *J. Am. Chem. Soc.* **1958**, *80*, 2421.
 (40) Saunders, W. H., Jr.; Glaser, R. *J. Am. Chem. Soc.* **1960**, *82*, 3586.
 (41) Lee, C. C.; Noszko, L. *Can. J. Chem.* **1966**, *44*, 2491.
 (42) Shiner, V. J., Jr.; Dowd, W. *J. Am. Chem. Soc.* **1971**, *93*, 1029.
 (43) Harris, J. M.; Hall, R. E.; Schleyer, P. v. R. *J. Am. Chem. Soc.* **1971**, *83*, 2553.
 (44) (a) Bron, J.; Stothers, J. B. *Can. J. Chem.* **1968**, *46*, 1435; (b) *Ibid.* **1968**, *46*, 1825; (c) *Ibid.* **1969**, *47*, 2506.
 (45) Halevi, E. A., In "Progress in Physical Organic Chemistry", Cohen, S. G.; Streitwieser, A., Jr.; Taft, R. W., Eds.; Interscience: New York, 1963; Vol. 1.
 (46) Hartshorn, S. R.; Shiner, V. J., Jr. *J. Am. Chem. Soc.* **1972**, *94*, 9002.

(47) Hehre, W. J. *J. Am. Chem. Soc.* **1972**, *94*, 5919.

(48) Snyder, E. J., *J. Am. Chem. Soc.* **1970**, *92*, 7529.

(49) Stern, M. J.; Wolfsberg, M. *J. Chem. Phys.* **1966**, *45*, 4105.

(50) "Table of Interatomic Distances and Configurations in Molecules and Ions", Special Publications No. 11 and 18, The Chemical Society (London), 1958, 1965.

β carbons (C_1 and C_2 , respectively), and trigonal planar geometry was assumed about the phenyl-1 position (C_6). All bond orders, n , were assumed to be unity in the reactant except for the aromatic C-C bonds, for which the bond order, n_3 , was taken as 1.65 to represent the aromatic stabilization of the phenyl ring.⁵¹

The bond lengths and bond angles for the transition-state models were related to those of the reactant by means of semiempirical and empirical relations involving the bond orders assigned to the TS model. Bond lengths for the reacting bonds 1-5 were adjusted by a revised version of Pauling's bond order-bond length expression⁵² (eq 4); all nonreacting bonds were assumed to have bond

$$r = r^0 - 0.30 \ln n \quad (4)$$

orders of unity as in the reactant. The bond angles within the cyclic structure formed by the transferring phenyl group and the α and β carbons (ϕ_{126} , ϕ_{261} , and ϕ_{612}) are determined by the law of cosines, using the bond lengths calculated by eq 4 from the bond orders n_2 , n_3 , and n_4 . The other angles were related to the bond orders and to these angles by expressions designed to simulate the changes between reactant and transition state consistent with the expected hybridization changes.²⁰ Thus, the CCC angle ϕ_{728} changes from tetrahedral (T_d) to 120° (eq 5) and θ_2 changes from

$$\phi_{728} = 120.0 - 10.53n_4 \quad (5)$$

54.7° ($T_d/2$) to 0° (eq 6) as the hybridization at the β carbon

$$\phi_2 = \phi_{126}n_4/(n_2 + n_4) \quad (6)$$

changes from sp^3 to sp^2 . Similarly, the HCH angle ϕ_{415} and the angle ϕ_1 change from T_d and $T_d/2$, to 120° and 0° , to T_d and $-T_d/2$, respectively, as the leaving group departs and the expected inversion at the α carbon occurs; these changes are represented by eq 7 and 8.

$$\phi_{415} = 120.0 - 10.53|n_1 - n_3| \quad (7)$$

$$\theta_1 = (\phi_{312}n_1 - \phi_{612}n_3)/(n_1 + n_2 + n_3) \quad (8)$$

The angle to the leaving group (ϕ_{312}) was assumed to remain tetrahedral during the reaction, while the angle θ_3 between the plane of the phenyl ring and the C_β -phenyl bond increased (from 0° in the reactant), according to eq 9. Even though the calculated

$$\theta_3 = \phi_{261}n_3/(n_3 + n_4) \quad (9)$$

KIE are not very sensitive to the geometrical parameters of the models (i.e., to the exact form of eq 4-9), eq 4-9 provide physically reasonable estimates of the expected structural changes and a systematic way of relating them to the orders n_1 - n_5 of the reacting bonds.

A simple valence force field (SVFF, diagonal potential energy matrix) was used for both the reactant and the TS models except that one or two interaction force constants (off-diagonal potential energy matrix elements) were used to generate a zero or imaginary reaction coordinate frequency (ν_L^{\ddagger}) in the transition state (vide infra).

Standard force constants,⁵³ F^0 , were used for the reactant model. Force constants for the TS were related to those of the reactant model by empirical relations. Stretching force constants for each reacting bond 1-5 in the TS models were calculated from the Pauling-Badger relation,⁵⁴ eq 10, where n_i is the order of the

$$F_{ii} = n_i F_{ii}^0 \quad (10)$$

(51) Coulson, C. A., "Valence", 2nd ed.; Oxford University Press: London, 1961, p 269.

(52) Pauling, L. *J. Am. Chem. Soc.* **1947**, *69*, 542; the coefficient of 0.30 in eq 4 is a revised value (from 0.26) obtained by least-squares fit to data in ref 50.

(53) (a) Wilson, E. B., Jr.; Decius, J. C.; Cross, P. C. "Molecular Vibrations"; McGraw-Hill: New York, 1955, pp 175-176; (b) Herzberg, G. "Molecular Spectra and Structure, Part II: Infrared and Raman Spectra of Polyatomic Molecules"; Van Nostrand: Princeton, NJ, 1945; (c) Schachtschneider, J. H., Snyder, R. G. *Spectrochim. Acta* **1963**, *19*, 117; Snyder, R. G., Schachtschneider, J. H. *J. Mol. Spectrosc.* **1969**, *30*, 290; *Spectrochim. Acta* **1965**, *21*, 169.

Table IV. Structural Parameters^a and Force Constants^b

bond stretch	acyclic reactant model		cyclic TS model	
	r_i^0	F_{ii}^0	r_i^c	F_{ii}^d
C-C	1.537	4.5	$1.537 - 0.3 \ln(n_{C-C})$	$4.5n_{C-C}$
C-C _{Ph}	1.5075	5.0	$1.5075 - 0.3 \ln(n_{C-C_{Ar}})$	$5.0n_{C-C_{Ar}}$
C _{Ph1} -C _{Ph2}	1.387 ^e	7.425 ^f	$1.537 - 0.3 \ln(n_{C_{Ar}-C_{Ar}})$	$4.5n_{C_{Ar}-C_{Ar}}$
C-H	1.094	5.0	1.094	5.0
C-O	1.430	5.3	$1.430 - 0.3 \ln(n_{C-O})$	$5.3n_{C-O}$

angle bend	acyclic reactant model		cyclic TS model	
	angle	F_{bend}^0	angle	F_{bend}^d
C ₁ -C _j -C _k	109.5	1.00	g	$1.0(n_{C_1-C_j}n_{C_j-C_k})^{1/2}g_\alpha$
H-C-O	109.5	0.75 ^h	g	$0.75(n_{C-O})^{1/2}g_\alpha$
C-C-H	109.5	0.65	g	$0.65(n_{C-C})^{1/2}g_\alpha$
H-C-H	109.5	0.55		
out-of-plane wag	0.0	0.20		
torsion ⁱ (C-C)		0.072		

^a Reference 51. Bond distances are given in angstroms, bond angles in degrees. ^b Reference 54. ^c See eq 4 of text. ^d See eq 10-12 of text. Units are md/Å for stretching and md·Å/rad² for bending force constants. ^e Calculated by the use of eq 4 of text with $r_i^0 = 1.537$ and $n = 1.65$. ^f Calculated by the use of eq 10 of text with $F_{ii}^0 = 4.5$ and $n = 1.65$. ^g See eq 5-9 of text. ^h 0.90 instead of 0.75 was used as F_{ii}^0 for product-like transition state models; this corrects the insufficiency of the g_α function at a range where α is smaller than 90° . ⁱ One torsional coordinate was used to describe torsion about each C-C bond.⁵⁵

bond and F_{ii}^0 is the standard (reactant value) force constant for a single bond i . Angle bending force constants in the TS were calculated from eq 11²⁰ where $F^0(T_d)$ is the standard (reactant

$$F_\alpha = g_\alpha(n_i n_j)^{1/2} F^0(T_d) \quad (11)$$

value) angle bending force constant for a tetrahedral angle formed by adjacent single bonds i and j , and g_α is a geometry or hybridization factor given by eq 12. The value of g_α is unity for

$$g_\alpha = 1.39 + 1.17 \cos \alpha \quad (12)$$

$\alpha = T_d = 109.47^\circ$ and decreases as α increases. Torsional and out-of-plane bending force constants occur only for the acyclic reactant model.

Equations 4-12 are to be regarded simply as a basis for producing TS models which have physically reasonable structures and force constants for the bond orders assigned to the model. The relations are calibrated with stable molecules and are believed to be qualitatively correct. Changes in the equations would lead to quantitative changes in the TS (i.e., changes in bond angles, lengths, and orders) for which calculated KIE agree with experimental values, but it is not expected that qualitative changes in the nature of the TS would result. Structural parameters and valence force constants for both the reactant and TS models are summarized in Table IV.

The TS will have a zero (or imaginary) frequency for one normal mode, corresponding to reaction coordinate motion, if the determinant of the TS force constant matrix is zero (or negative)

$$|F^{\ddagger}| \leq 0 \quad (13)$$

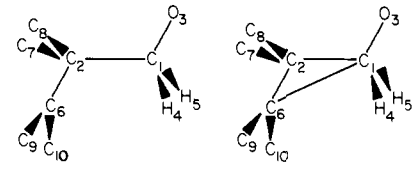
The reaction coordinate approximates a simple bond rupture of

(54) Johnston, H. S. "Gas Phase Reaction Rate Theory", Ronald Press: New York, 1966; Chapter 4.

(55) Williams, I. H., McKenna, J., Sims, L. B. *J. Mol. Struct.* **1979**, *55*, 147.

(56) Johnston, H. S.; Bonner, W. A.; Wilson, D. J. *J. Chem. Phys.* **1957**, *26*, 1002.

Table V. Internal Coordinates for Acyclic and Cyclic Model

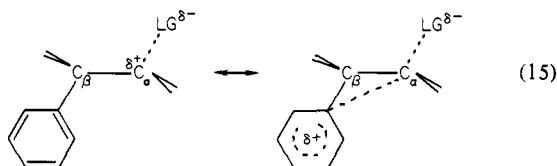


acyclic model		cyclic model	
$R_1 = \Delta r_{1,2}$	$R_{13} = \Delta \phi_{3,1,4}$	$R_1 = \Delta r_{1,2}$	$R_{13} = \Delta \phi_{3,1,4}$
$R_2 = \Delta r_{1,3}$	$R_{14} = \Delta \phi_{3,1,5}$	$R_2 = \Delta r_{1,3}$	$R_{14} = \Delta \phi_{3,1,5}$
$R_3 = \Delta r_{1,4}$	$R_{15} = \Delta \phi_{1,2,6}$	$R_3 = \Delta r_{1,4}$	$R_{15} = \Delta \phi_{1,2,7}$
$R_4 = \Delta r_{1,5}$	$R_{16} = \Delta \phi_{1,2,7}$	$R_4 = \Delta r_{1,5}$	$R_{16} = \Delta \phi_{1,2,8}$
$R_5 = \Delta r_{2,6}$	$R_{17} = \Delta \phi_{1,2,8}$	$R_5 = \Delta r_{2,6}$	$R_{17} = \Delta \phi_{6,2,7}$
$R_6 = \Delta r_{2,7}$	$R_{18} = \Delta \phi_{6,2,7}$	$R_6 = \Delta r_{2,7}$	$R_{18} = \Delta \phi_{6,2,8}$
$R_7 = \Delta r_{2,8}$	$R_{19} = \Delta \phi_{6,2,8}$	$R_7 = \Delta r_{2,8}$	$R_{19} = \Delta \phi_{2,6,9}$
$R_8 = \Delta r_{6,9}$	$R_{20} = \Delta \phi_{2,6,9}$	$R_8 = \Delta r_{6,9}$	$R_{20} = \Delta \phi_{2,6,10}$
$R_9 = \Delta r_{6,10}$	$R_{21} = \Delta \phi_{2,6,10}$	$R_9 = \Delta r_{6,10}$	$R_{21} = \Delta \phi_{6,1,4}$
$R_{10} = \Delta \phi_{4,1,5}$	$R_{22} = \Delta \gamma_{2,6,9,10}$	$R_{10} = \Delta r_{1,6}$	$R_{22} = \Delta \phi_{6,1,5}$
$R_{11} = \Delta \phi_{2,1,4}$	$R_{23} = \Delta \tau_{1,2}$	$R_{11} = \Delta \phi_{2,1,4}$	$R_{23} = \Delta \phi_{1,6,9}$
$R_{12} = \Delta \phi_{2,1,5}$	$R_{24} = \Delta \tau_{2,6}$	$R_{12} = \Delta \phi_{2,1,5}$	$R_{24} = \Delta \phi_{1,6,10}$

bond *i* if this condition is satisfied by setting $F_{ij} \leq 0$; a concerted motion of bonds *i* and *j* in the reaction coordinate is implied if an interaction constant f_{ij} is introduced, such that $f_{ij}^2 \geq F_{ii}F_{jj}$ in order to satisfy eq 13. A realistic concerted reaction coordinate motion for the present system was achieved by the use of one or more off-diagonal force constants coupling adjacent bonds *i* and *j* in the force constant matrix of the TS. These interaction force constants were related to the stretching force constants by eq 14.⁵⁷

$$f_{ij} = A_{ij}(F_{ii}F_{jj})^{1/2} \quad (14)$$

For most of the calculations, a single interaction constant coupling bonds 1 and 3 was employed (eq 13 then becomes $1 - A_{13}^2 \leq 0$); for $A_{13} \geq 1.0$, this corresponds to an S_N2 -like asymmetric reaction coordinate motion at C_α with the forming C_α -phenyl bond (bond 3) displacing the rupturing C_α -leaving group bond (bond 1). Later calculations employed two additional small interaction force constants (f_{35}) to represent the C_α -phenyl interaction (bond 3) occurring at the expense of the π -electron density of the ortho bonds of the phenyl ring (bonds 5), e.g., a possible resonance interaction between the α -carbon and the migrating phenyl group, as shown in eq 15. In this case, the requirement for a zero or



imaginary reaction coordinate frequency generated by the two interaction constants f_{13} and f_{35} (both given by eq 14) is found from expansion of the determinantal eq 13 to be given by relation 16 where the barrier curvature parameter D corresponds to a

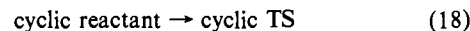
$$(1 - A_{13}^2 - 2A_{35}^2) = D \leq 0 \quad (16)$$

reaction coordinate frequency (ν_L^\ddagger) that is zero ($D = 0$, flat barrier) or imaginary ($D < 0$, curved barrier) and corresponds to an asymmetric concerted motion of bonds 1, 3, and 5 for $A_{13} \geq 1$ and $A_{35} \geq 1$.

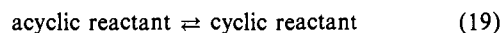
The overall reaction can be represented by eq 17. A kinetically complete set of 24 internal coordinates can easily be defined by using the rules of Decius⁵⁷ for the acyclic reactant (see Table V).

The cyclic TS requires the addition of a new bond between C_α and the Ph-1 ring carbon and several additional bending coordinates between this new bond and the adjacent

bonds, thus introducing several redundant coordinates. The problem of redundant coordinates in cyclic TS has been treated in general by Keller and Yankwich,⁵⁸ who provide a method for solving this problem by (i) eliminating some coordinates or by (ii) transforming F^\ddagger to correspond to a nonredundant G . The methods given⁵⁸ for procedure ii are not adapted readily to the current problem; fortunately method i can be applied readily since the rules of Decius⁵⁷ allow a choice of 24 kinematically complete coordinates for the cyclic TS (Table V). There is a further difficulty with these coordinates, however, since the calculation of KIE using cutoff models requires that the internal coordinates retained in the reactant and TS cutoff models be the same;⁴⁹ this is not possible using an acyclic reactant model and the cyclic TS model required to simulate a concerted process with neighboring group participation. The solution adopted was to "simulate" the reactant by using a cyclic reactant model in which the $C_1C_2C_6$ angle bending force constant is represented by a "stretching" force constant between C_1 and C_6 . Since a change in the (nonbonded) distance C_1-C_6 in the reactant is related by geometry to a change in the $C_1C_2C_6$ angle, it is possible to derive an analytical relation between the two force constants; however, the torsional and out-of-plane coordinates of the acyclic model are related to new angle bending coordinates of the cyclic model also, so that the relationship between the corresponding acyclic and cyclic force fields of the reactant model is not simple. The KIE calculated by reaction 18 will correctly represent those for the overall process



(eq 17), provided that the isotope effects for the "pseudo equilibrium" (eq 19) are unity for all labeled positions.



Since KIE are determined by the relative changes in structure and force constants between reactant and TS, the actual structural parameters and force constants assumed for the reactant do not seriously affect the calculated KIE; any physically reasonable values for the reactant (derived or estimated from experimental data if possible, of course) can be used to obtain reliable KIE. Therefore, a physically reasonable set of force constants for the acyclic reactant model was chosen from experimental data and standard sources of force constants.⁵³ A set of force constants for the cyclic reactant model which produced null isotope effects for labeling at C_α , C_β , and C_{Ph-1} and at D_α for the pseudoequilibrium (eq 19) was then found by trial and error. The force constants for the cyclic reactant model were then used as the "standard" force constants in eq 10-12 to yield a force field for the cyclic TS models.

Frequencies and principal moments of inertia were calculated for the various isotopic reactant and TS models by using a version⁵⁹ of the normal coordinate and vibrational analysis program of Gwinn.⁶⁰ The KIE were then calculated by using the expressions of Bigeleisen and Mayer,⁶¹ given in the notation of Wolfsberg and Stern⁶² in eq 20, where the asterisk denotes the heavier isotopic

$$\text{KIE} = k/k^* = \text{MMI} \times \text{EXC} \times \text{ZPE} \quad (20)$$

molecule. The factors represent the ratio of TS to reactant values of molecular masses and moments of inertia (MMI), excited vibrational states (EXC), and zero-point energy (ground vibrational state, ZPE). The ratio of isotopic reaction coordinate frequencies, $(\nu_L/\nu_L^*)^\ddagger$, can be obtained either directly from the program (if ν_L^\ddagger is imaginary) or by means of the Teller-Redlich products rule,⁶² which gives eq 21, where VP is the vibrational frequency product ratio.⁶²

$$(\nu_L/\nu_L^*)^\ddagger = \text{MMI}/\text{VP} \quad (21)$$

(58) Keller, J. H.; Yankwich, P. E. *J. Am. Chem. Soc.* **1974**, *96*, 2303.

(59) Sellers, H. L.; Sims, L. B.; Schafer, L.; Lewis, D. E. *J. Mol. Struct.* **1977**, *41*, 149.

(60) Gwinn, W. D. *J. Chem. Phys.* **1971**, *55*, 477.

(61) (a) Bigeleisen, J. *J. Chem. Phys.* **1949**, *17*, 675; (b) Bigeleisen, J.; Mayer, M. G. *J. Chem. Phys.* **1947**, *15*, 261.

(57) Decius, J. C. *J. Chem. Phys.* **1949**, *17*, 1315.

Table VI. Bond Orders and Calculated Kinetic Isotope Effects for the Parent Compound, Assuming $A = 1.00$ and $n_{\alpha-\beta} = 1.00$

$n_{\alpha-O}$	$n_{\alpha-Ph}$	$n_{\beta-Ph}$	$n_{Ph_1-Ph_2}$	$\alpha-^{14}C$	$\alpha-D_2$	$\beta-^{14}C$	Ph- ^{14}C
0.05	0.15	1.0	1.35	1.1019	1.4049	1.0089	1.0112
0.05	0.20	0.95	1.20	1.0950	1.3575	1.0118	1.0206
0.05	0.25	1.0	1.30	1.0885	1.3217	1.0084	1.0050
0.05	0.29	0.95	1.20	1.0842	1.2945	1.0117	1.0123
0.08	0.29	0.95	1.00	1.0917	1.2259	1.0134	1.0297
0.09	0.29	0.95	1.05	1.0935	1.2074	1.0135	1.0256
0.05	0.32	0.95	1.20	1.0810	1.2770	1.0118	1.0097
0.10	0.15	1.0	1.375	1.1084	1.2885	1.0112	1.0118
0.10	0.20	1.0	1.35	1.1041	1.2493	1.0105	1.0077
0.10	0.25	1.0	1.20	1.0990	1.2155	1.0106	1.0142
0.10	0.30	1.0	1.20	1.0938	1.1864	1.0104	1.0094
0.10	0.32	0.95	1.10	1.0920	1.1739	1.0136	1.0187
0.15	0.10	1.0	1.375	1.1086	1.2552	1.0130	1.0222
0.15	0.10	0.95	1.40	1.1061	1.2510	1.0159	1.0208
0.15	0.15	1.0	1.325	1.1079	1.2076	1.0123	1.0174
0.15	0.25	1.0	1.25	1.1034	1.1434	1.0116	1.0117
0.15	0.32	0.95	1.05	1.0982	1.1052	1.0148	1.0242
0.20	0.05	1.0	1.375	1.0930	1.2447	1.0151	1.0264
0.20	0.05	0.95	1.40	1.0915	1.2414	1.0173	1.0264
0.20	0.075	1.0	1.35	1.0961	1.2144	1.0134	1.0251
0.20	0.10	1.0	1.35	1.1007	1.1907	1.0130	1.0224
0.20	0.15	1.0	1.30	1.1051	1.1507	1.0126	1.0206
0.21	0.06	1.0	1.425	1.0991	1.2190	1.0135	1.0209
0.225	0.05	1.0	1.35	1.0864	1.2146	1.0138	1.0272
0.225	0.075	1.0	1.35	1.0935	1.1892	1.0132	1.0253
0.25	0.05	1.0	1.35	1.0839	1.1920	1.0135	1.0273

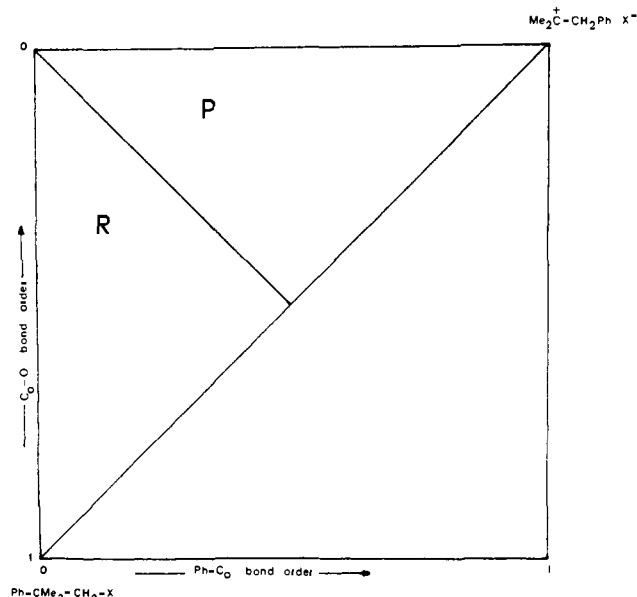
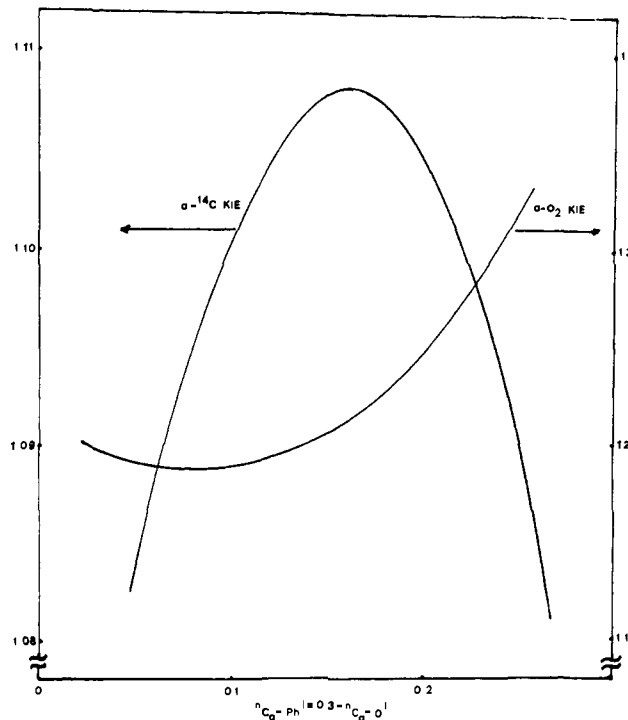


Figure 4. Transition state map for phenyl rearrangement step of neophyl solvolysis.

Discussion

Calculations were carried out for the parent compound by using eq 18, employing transition-state models in which the bond loss at the α carbon occasioned by departure of the leaving group, $(1 - n_{\alpha-O})$, is only partially compensated for by bond formation to the migrating phenyl group, $(n_{\alpha-Ph})$. These two coordinates can be used as the axes for the O'Ferrall-Jencks reaction diagram shown in Figure 4; the TS models considered lie in the left-hand upper half of this diagram. With respect to bonding changes at the α position, the transition states can be characterized as reactant-like (R) if $n_{\alpha-O} > n_{\alpha-Ph}$ and product-like (P) if $n_{\alpha-O} < n_{\alpha-Ph}$, as indicated in Figure 4. For a TS with a reaction coordinate that corresponds to an S_N2 -like motion at C_α , there are six independent parameters: $n_{\alpha-O}$ (or n_1), $n_{\alpha-\beta}$ (or n_2), $n_{\alpha-Ph}$ (or n_3), $n_{\beta-Ph}$ (or n_4), $n_{Ph_1-Ph_2}$ (or n_5), and the reaction coordinate parameter A (or A_{13}

Figure 5. Trends in calculated $\alpha-^{14}C$ and $\alpha-D_2$ kinetic isotope effects as a function of C_α -leaving group and C_α -phenyl bond orders. For this case, $n_{C_\alpha-Ph} + n_{C_\alpha-O} = 0.3$, $n_{\alpha-\beta} = 1.0$, $A = 1.0$ as in Table VI.

of eq 14); other parameters of the model are determined by eq 4-12.

Since there are only four measured isotope effects, there is no unique solution, but a family of solutions can be found. For example, if the constraints $n_{\alpha-\beta} = 1$ (no double bond formation in the TS) and $A = 1.0$ (flat barrier, with zero reaction coordinate frequency) are imposed, KIE can be calculated as functions of the remaining four bond orders, as in Table VI. Of the four KIE calculated, the $\alpha-^{14}C$ and the $\alpha-D_2$ effects are determined by the $n_{\alpha-O}$ (or n_1) and $n_{\alpha-Ph}$ (or n_3) bond orders and are relatively insensitive to the $n_{\beta-Ph}$ (or n_4) and $n_{Ph_1-Ph_2}$ (or n_5) bond orders since bonds 4 and 5 are two bonds removed from the labeled α -carbon. Thus, trends in these two isotope effects as n_1 and n_3 are changed

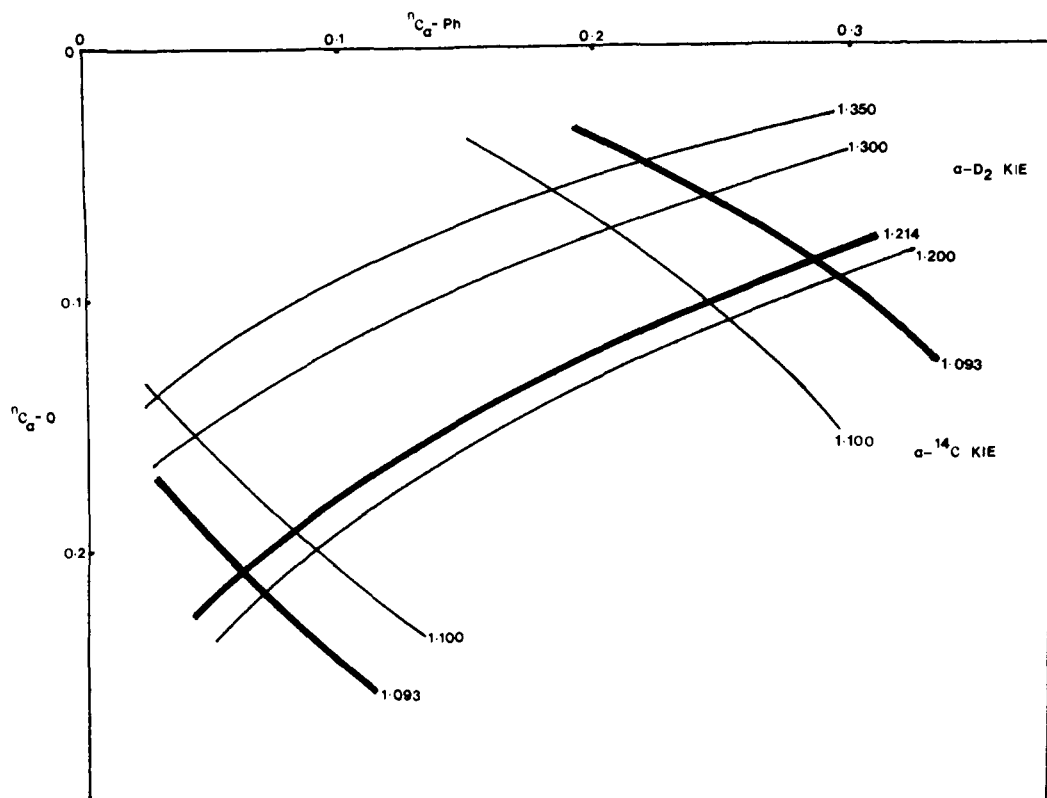


Figure 6. Constant isotope effect curves for α - ^{14}C and α - D_2 kinetic isotope effects for the parameters given in Table VI.

Table VII. Combinations of $n_{\alpha-\beta}$ and A for which KIE Calculations Were Carried Out^a

A	$n_{\alpha-\beta}$								
	1.0		1.1		1.2		1.3		
	R	P	R	P	R	P	R	P	
1.00	+	+	+	+	+	+	+	+	+
1.25	+	-	+	+	+	+	-	+	+
1.50	-	-	+	-	-	+	-	+	+
1.75	-	-	-	-	-	+	-	-	+
2.00	-	-	-	-	-	-	-	-	+

^a +(-) means that there is (is not) a reasonable reactant-like (R) or product-like (P) transition-state structure which reproduces the experimentally observed KIE.

are especially revealing. For cases where $n_1 + n_3 = \text{a constant}$, K (where $1.0 - K$ represents the fraction of the C_α -leaving group bond loss not compensated for by bonding to the migrating phenyl group), Figure 5 shows that the α - ^{14}C and α - D_2 KIE go through a maximum and minimum, respectively, when plotted against the C_α -O bond order. A bell-shaped behavior for the α - ^{14}C KIE has been calculated for $\text{S}_{\text{N}}2$ reactions¹⁹ and experimentally confirmed.⁶⁴ The calculated α - ^{14}C KIE curve in Figure 5 intersects at two points with the experimental value of the KIE (1.093), indicating two TS models (one in the R and one in the P region of Figure 4) which reproduce the experimental value. These two TS correspond to two points in the $n_{\alpha-\text{O}}, n_{\alpha-\text{Ph}}$ plane of Figure 6; two points for TS which reproduce the α - D_2 KIE are obtained by the same procedure. Plots such as Figure 5 for values of $0.0 < K < 1.0$ produce a family of TS which reproduce the α - ^{14}C or the α - D_2 KIE; these TS map onto Figure 6 as the heavy contour lines. Similar procedures lead to the light contour lines of Figure 6, corresponding to TS which produce other indicated values of the KIE.

The intersection of the two heavy lines in Figure 6 represents a TS which simultaneously reproduces the experimental values of both the α - ^{14}C and the α - D_2 KIE. The values of $n_{\alpha-\text{O}}$ and $n_{\alpha-\text{Ph}}$ for this TS were then held constant and the bond order $n_{\beta-\text{Ph}}$ was varied so as to reproduce the observed β - ^{14}C KIE; then the bond order $n_{\text{Ph}_1-\text{Ph}_2}$ was varied to reproduce the observed $\text{Ph}-I$ - ^{14}C KIE.

Table VIII. Structural Parameters of Successful^a Transition State Models for the Parent Compound, Neophyl Brosylate

A	$n_{\alpha-\beta}$	$n_{\alpha-\text{Ph}}$	$n_{\alpha-\text{O}}$	$n_{\beta-\text{Ph}}$	$n_{\text{Ph}_1-\text{Ph}_2}$
P region					
1.00	1.00	0.290	0.085	0.950	1.075
1.00	1.10	0.240	0.090	0.850	1.200
1.00	1.20	0.210	0.090	0.800	1.275
1.00	1.30	0.165	0.095	0.700	1.400
1.25	1.10	0.340	0.065	0.830	1.125
1.25	1.20	0.300	0.065	0.750	1.225
1.25	1.30	0.240	0.065	0.650	1.375
1.50	1.10	0.390	0.050	0.800	1.075
1.50	1.20	0.350	0.050	0.750	1.175
1.50	1.30	0.280	0.053	0.650	1.350
1.75	1.20	0.380	0.047	0.750	1.150
1.75	1.30	0.310	0.047	0.650	1.320
2.00	1.20	0.415	0.040	0.750	1.100
2.00	1.30	0.325	0.040	0.650	1.250
R region					
1.00	1.00	0.065	0.210	1.000	1.375
1.00	1.10	0.070	0.180	0.900	1.450
1.00	1.20	0.080	0.160	0.850	1.500
1.00	1.30	0.090	0.135	0.750	1.550
1.25	1.00	0.050	0.230	1.000	1.450
1.25	1.10	0.055	0.200	0.900	1.500
1.25	1.20	0.065	0.175	0.850	1.600
1.50	1.10	0.040	0.220	0.900	1.575

^a Successful TS are those corresponding to + entries of Table VII.

This procedure yielded a TS with preselected $n_{\alpha-\beta}$ and A , but the other four bond orders were determined to fit the experimental KIE. The entire procedure was repeated for different values of $n_{\alpha-\beta}$ and A in the range $1.0 \leq n_{\alpha-\beta} \leq 1.3$ and $1.0 \leq A \leq 2.0$. Table VII gives the values of $n_{\alpha-\beta}$ and A which did (+) or did not (-) yield reactant-like (R entries) or product-like (P entries) TS which reproduce the experimental KIE. The bond orders for those TS which did reproduce the experimental KIE are listed in Table VIII and plotted on a reaction diagram in Figure 7. The figure indicates that the family of solutions corresponds to two fairly limited regions of R-like and P-like transition states; the R-like

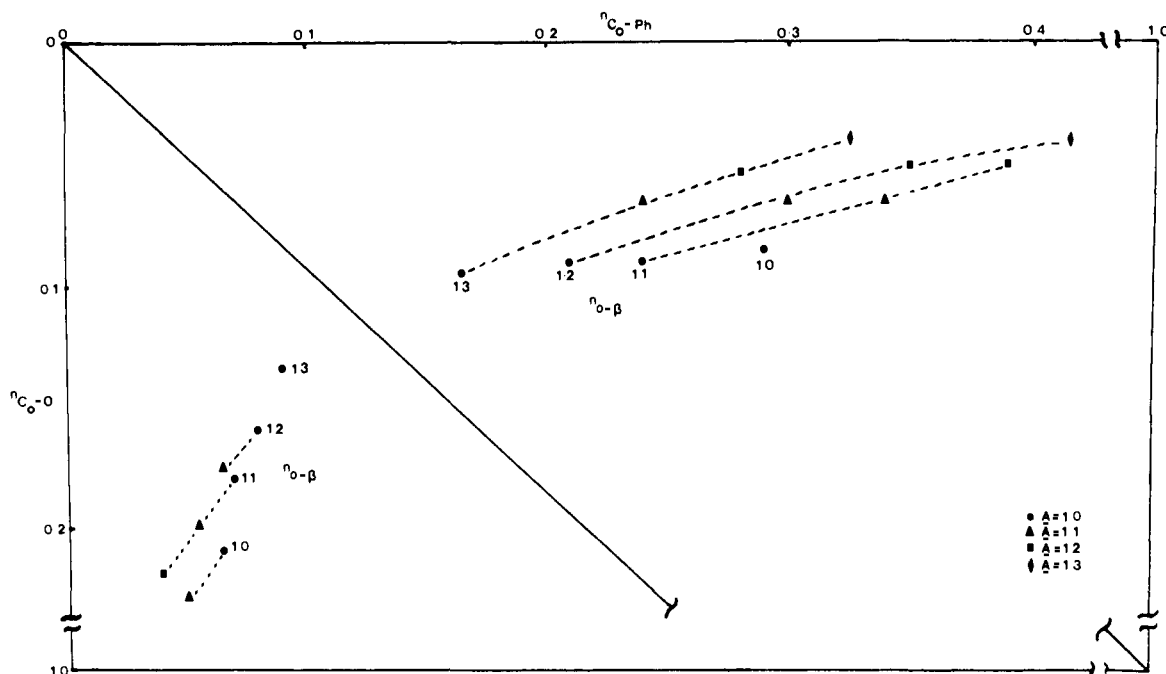


Figure 7. Transition-state map with transition states for the parent compound which reproduce experimental kinetic isotope effects for indicated values of $n_{\alpha-\beta}$ and A .

transition states are later shown to be unlikely for these processes. Therefore, for the parent compound, the most likely TS can be characterized as follows: (1) C_{α} -O bond rupture is much further advanced than is phenyl migration; (2) phenyl migration is far less than halfway complete, so that both the Ph-1 and the β -carbon positions are reactant-like; (3) at C_{α} , the bond order $n_{\alpha-Ph} > n_{\alpha-O}$, so that the TS is product-like at this center.

Calculations for the p - CH_3O and the p -Br compounds were carried out by using the same procedures and models as for the parent compound. In several of the calculations, the decrease in $n_{Ph_1-Ph_2}$ required to obtain agreement with the Ph-1- ^{14}C KIE was large, corresponding to an unrealistic TS structure with loss of aromaticity in the ring and a decreased bond order at the Ph-1 position, which is not demanded by the weak C_{α} -Ph interaction and the slightly weakened C_{β} -Ph bond deduced from the α - and β - ^{14}C KIE. We feel, therefore, that it is not possible to adequately explain the Ph-1- ^{14}C KIE by bonding changes alone. The other factor which can affect the KIE is the reaction coordinate motion, and we therefore explored the addition of a reaction coordinate parameter B (or A_5 of eq 14) representing coupling between the $C_{Ph_1}-C_{Ph_2}$ and the C_{α} -phenyl bonds. As expected, the addition of B had a large effect upon the Ph-1- ^{14}C KIE, but very little effect on the other KIE; a value of $B = 0.3$ caused an increase of 1.15% in the Ph-1- ^{14}C KIE and 0.03% in the β - ^{14}C KIE and a decrease of 0.05% and 0.3% in the α - ^{14}C and the α - D_2 KIE, respectively. Values of A and n_1 - n_4 from the earlier calculations were retained, and B and n_5 (i.e., $n_{Ph_1-Ph_2}$) were adjusted so that the experimental Ph-1- ^{14}C KIE was reproduced and n_5 was reasonable.

The TS areas for the unsubstituted and for the two substituted compounds are shown in Figure 8. There is a general shift of the P-like TS region toward the product and of the R-like TS region toward the reactant as the para substituent becomes more electron withdrawing. The shifts in TS structure as the substituent is changed become clearer if one compares TS within each region which are related in a reasonable way to one another, that is, TS whose properties (bond orders, reaction coordinate motion, ν_L^\ddagger , etc.) vary smoothly with substituent and for which the reaction coordinate frequency increases as the TS becomes more symmetrical with respect to the bonding about C_{α} , by analogy to S_N2

Scheme II

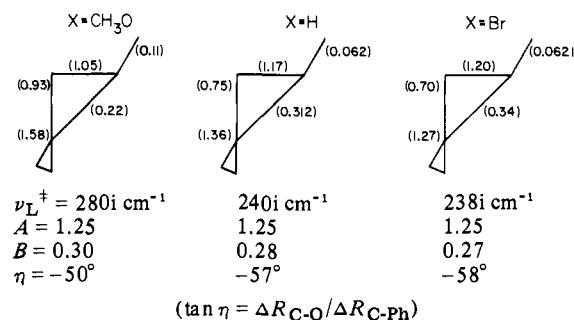


Table IX. Kinetic Isotope Effects in the Acetolysis of Substituted Neophyl Brosylates at $75^\circ C^a$

substituent	α - ^{14}C	β - ^{14}C	Ph-1- ^{14}C	α - D_2
p - CH_3O	1.110 1.111 ^b	1.009	1.007 1.006 ^c	1.198 1.198 ^d
p -H	1.094 1.093 \pm 0.003	1.014 1.014 \pm 0.001 ^b	1.023 1.023 \pm 0.001 ^b	1.212 1.214 \pm 0.002 ^b
p -Br	1.090 1.090 ^b	1.017	1.031 1.032 ^c	1.188 1.188 ^d

^a Upper entries, calculated values for TS models in Scheme II; lower entries, experimental values. ^b Table II. ^c Estimated from data in ref 11. ^d Estimated from data in ref 30.

processes.⁶⁵ No series of R-like TS could be found which satisfied these conditions; on the other hand, P-like TS which satisfy the above conditions are easily found. Figure 9 shows the trend of bond orders with the Hammett σ parameter for the series of TS shown in Scheme II. For the TS in Scheme II, all are reactant-like at C_{β} and at the Ph-1 positions, but are increasingly product-like at C_{α} as the substituent changes from p - OCH_3 to p -Br. This is clearly indicated by the parameter η (the relative change in C_{α} -O and C_{α} -Ph bonds in the TS); a symmetrical TS (about C_{α}) is characterized by $\eta = -45^\circ$, whereas $\eta = 0^\circ$ and $\eta = -90^\circ$ correspond to very reactant-like and product-like TS,

(63) Redlich, O. Z. *Phys. Chem., Abt. B* **1935**, *28*, 371; Teller, E., 1934, quoted by Angus, W. R.; Bailey, C. R.; Hale, J. B.; Ingold, C. K.; Leckie, A. H.; Raisin, C. G.; Thompson, J. W.; Wilson, C. L. *J. Chem. Soc.* **1936**, 971.
 (64) Yamataka, H.; Ando, T. *Tetrahedron Lett.* **1975**, 1059.

(65) Buddenbaum, W. E.; Shiner, V. J. Jr., *Can. J. Chem.* **1976**, *54*, 1146.

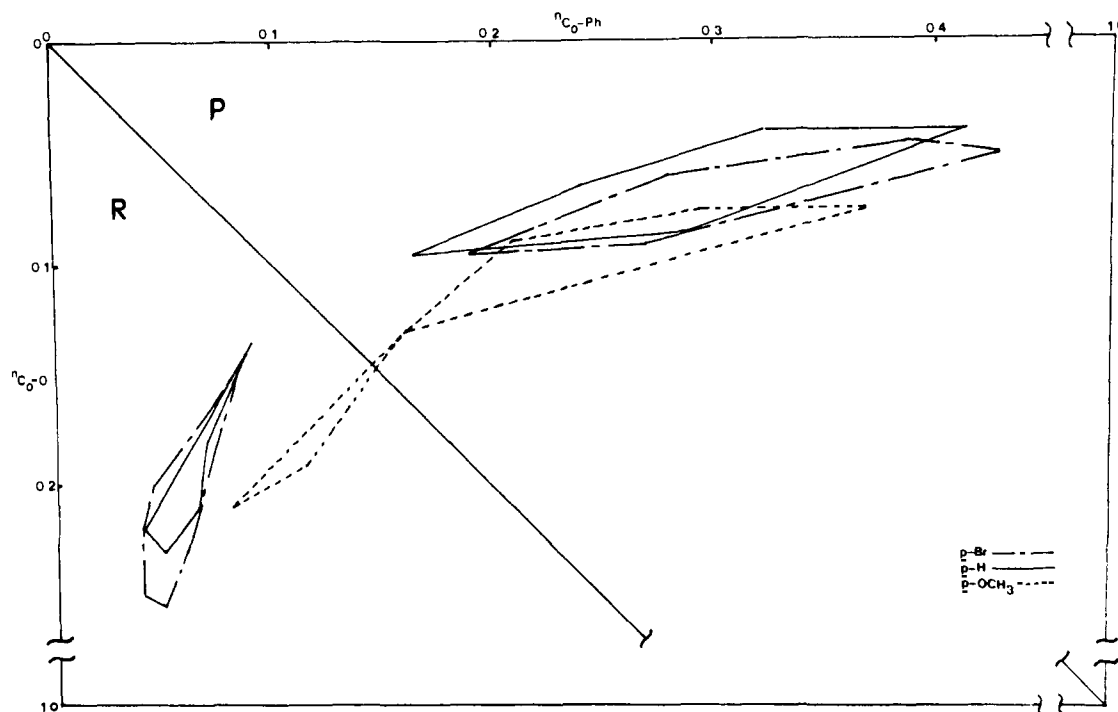


Figure 8. Transition-state map with regions where transition states reproduce experimental kinetic isotope effects for various combinations of $n_{\alpha-\beta}$ and A .

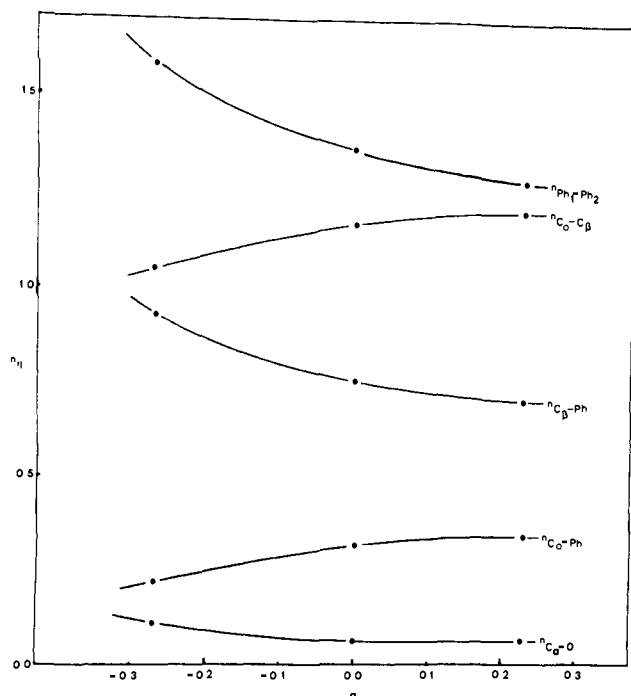


Figure 9. Trends in bond orders as a function of the Hammett σ value for transition states selected from the P regions of Figure 8.

respectively.⁶⁵ Figure 10 shows the TS structures on a reaction diagram. The overall agreement with experiment is given in Table IX.

The series of TS in Scheme II and in Figures 8–10 is not unique. A different set could be obtained by using different values of A , for example. However, similar changes in the TS for all substituents would be necessary if A were changed. For example, for $A = 1.50$, the C_{α} -Ph bond order would be increased by ~ 0.02 and the C_{α} -O bond order would be decreased by ~ 0.01 from the above series in order to retain agreement with the experimental α -¹⁴C KIE; very similar changes would be required for the p -OCH₃ and p -Br compounds. Note that the bond orders change very slowly and that the trends in KIE are in large measure unaffected

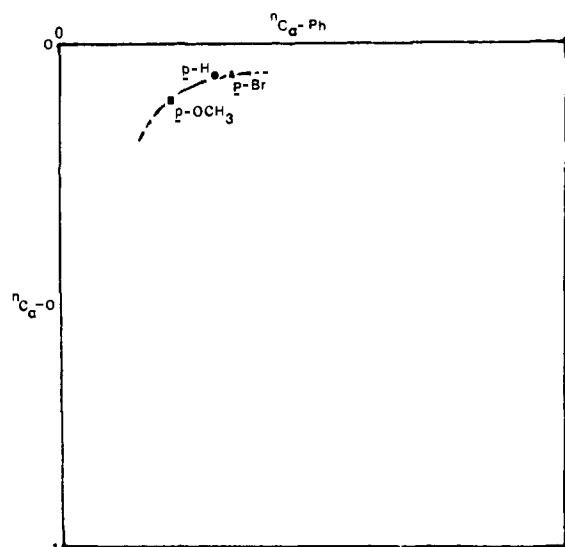
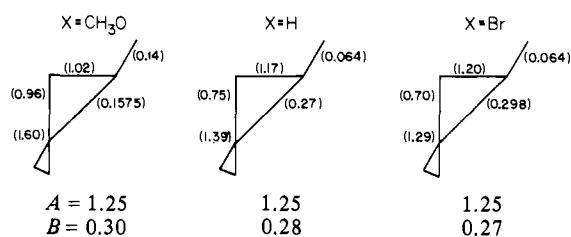


Figure 10. Transition-state map showing the position of the transition states which produce the best overall agreement with experiment.

by these changes in reaction coordinate parameters. It seems clear that the nature of the TS deduced in these calculations would not differ significantly if additional data were available.

In order to assess the importance of the force field assumptions on the results, we investigated an alternative force field model. Stretching force constants are believed to be given adequately by the Pauling-Badger relation, eq 10, so that all stretching force constants were retained from the previous model. But several relations other than eq 11 have been suggested for bending force constants. Most do not contain any geometry factor analogous to g_{α} , which we believe to be of considerable importance.²⁰ However, eq 11 suggests that the bending force constant vanishes when the order of either of the subtending bonds, n_i or n_j , becomes zero. This is reasonable for those coordinates which vanish in this limit; but some angle-bending coordinates (ϕ_{169} and ϕ_{627} in the present model) become out-of-plane bending motions in this limit ($n_3 = n_{\alpha-\text{Ph}} = 0$ in the reactant and $n_4 = n_{\beta-\text{Ph}} = 0$ in the product for the neophyl brosylates). In order to account for a nonvanishing

Scheme III



force constant for out-of-plane coordinates, Saunders⁶⁶ has used relation 11' (with $g_\alpha = 1.0$) in calculations of KIE for elimination

$$F_\alpha = g_\alpha(n_i n_j) F_\alpha^0(T_d) + 0.235 \quad (11')$$

reactions. In the present model, eq 11', with g_α given by eq 12, was used for bending coordinates ϕ_{169} and ϕ_{627} , retaining the value of $F^0(T_d)$ from Table IV. For coordinates ϕ_{269} and ϕ_{127} , eq 11

(66) Saunders, W. H., Jr. *Chem. Scr.* 1975, 8, 82.

was used, but the value of $F^0(T_d)$ was increased by 0.235 over that in Table IV in order to account for the fact that sp^2 bending force constants are larger than the corresponding sp^3 values. All other force constants were the same as in the previous model. Despite the rather large differences in several force constants, the resulting TS models (Scheme III) differ significantly from those of Scheme II only in that the $C_\alpha-O$ bond is slightly less ruptured in the present case. Otherwise, the conclusions are essentially unchanged from the previous model, suggesting that the results are not seriously affected by the form of the empirical relations used to generate the TS force field.

Acknowledgment. Financial support of this research by the Japan Ministry of Education (Grant No. 747018) and by the U.S. National Science Foundation (Grant No. CHE 76-09809) is gratefully acknowledged.

Supplementary Material Available: Activity data for the results obtained in this study (12 pages). Ordering information is given on any current masthead page.

Mechanism of Disproportionation of Ascorbate Radicals

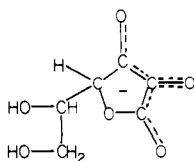
Benon H. J. Bielski,* Augustine O. Allen, and Harold A. Schwarz

Contribution from the Chemistry Department, Brookhaven National Laboratory, Upton, New York 11973. Received December 26, 1980

Abstract: Existing data on the kinetics of ascorbate radical decay, together with some new data on the effects of temperature, ionic strength, and presence of phosphate buffers, suggest a mechanism in which the ascorbate radical ion is in equilibrium with a dimer. This dimer reacts with hydrogen ion, or with other proton donors present including water and buffers (at rates depending upon their acid strengths), to form the disproportionation products ascorbate ion and dehydroascorbate acid.

The rate of spontaneous bimolecular decay of ascorbate radicals was first measured in 1960 in the course of a study of the kinetics of enzymatic oxidation of ascorbate.¹ In 1971, Bielski, Comstock, and Bowen² studied the reaction by pulse radiolysis, generating the radical by reaction of OH with ascorbate. They found that increasing the pH from 2 to 9 reduced the decay rate by a factor of 2000, and that at any given pH the rate increased with the concentration of added phosphate buffer.

The following year, a detailed study by Schöneshöfer³ appeared, which included spectroscopic evidence for several different radicals formed by the action of OH on ascorbic acid. He showed that this complication could be avoided by the addition of halide or thiocyanate ions to the ascorbate solution; e.g., $OH + Br^- \rightarrow BrOH \xrightarrow{-Br} OH^- + Br_2^-$, and Br_2^- reacts with ascorbate ion to form only the principal ascorbic acid radical I. Bielski et al.² had



I

reported that the extinction coefficient of the radical changed with pH, but this was an error resulting from the formation of different types of radicals from oxidation of ascorbate by OH; Schöneshöfer³

showed that when halide radicals were used as oxidants the extinction coefficient at 360 nm was essentially independent of pH. Fessenden, Schuler, and co-workers^{4,5} studied the reaction by electron spin resonance (ESR) spectra and verified that only I forms in the reaction of Br_2^- with ascorbate.

The ESR study⁴ showed that I is in the anionic form over the pH range 1-12 and protonates only at still lower pH. The great change in the radical decay rate between pH 3 and 9 is therefore not due to a change in the nature of the radical and must result from some kind of acid catalysis. To understand the mechanism of the reaction and the phosphate effect, we have recalculated some of the older results² and have obtained some new pulse-radiolysis data.

Experimental Section

L-Ascorbic acid was "certified ACS" grade from Fisher Scientific Co. Hydrochloric and sulfuric acids were Aristar distilled and phosphoric acid was MCB reagent grade. Other chemicals were Baker analyzed. Water, after distillation, was passed through a Millipore ultrapurification system.

Pulse radiolysis was carried out with 2 MeV electron beams from a Van de Graaff generator. Pulses were 2-5 μ s long; doses varied from 80 to 1700 rads. Radical concentrations were calculated from optical densities at 360 nm assuming an extinction coefficient of 3300 $M^{-1} cm^{-1}$.⁶

Solutions were 2×10^{-4} M in ascorbic acid and 0.02 M in KBr, and were saturated with N_2O at atmospheric pressure to convert solvated electrons to OH radicals. Runs with phosphate were always 0.0485 M in total phosphate, pH being adjusted by varying the relative amounts of H_2PO_4 , NaH_2PO_4 , and Na_2HPO_4 . The highest pHs were adjusted with KOH.

(1) Yamazaki, I.; Piette, L. H. *Biochim. Biophys. Acta* 1961, 50, 62.

(2) Bielski, B. H. J.; Comstock, D. A.; Bowen, R. A. *J. Am. Chem. Soc.* 1971, 93, 5624.

(3) Schöneshöfer, M. *Z. Naturforsch., B.* 1972, 27B, 649.

(4) Laroff, G. P.; Fessenden, R. W.; Schuler, R. H. *J. Am. Chem. Soc.* 1972, 94, 9062.

(5) Fessenden, R. W.; Verma, N. C. *Biophys. J.* 1978, 24, 93.

(6) Schuler, R. H. *Radiat. Res.* 1977, 69, 417.